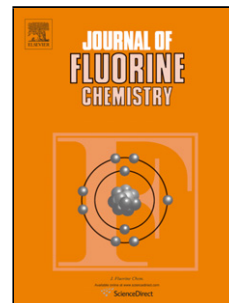


# Journal Pre-proof

Laser induced dielectric breakdown for synthesis of chlorofluorosilanes

P.G. Sennikov, I.B. Gornushkin, A.A. Ermakov, R.A. Kornev, V.E. Shkrunin, V.S. Polyakov



PII: S0022-1139(20)30390-0  
DOI: <https://doi.org/10.1016/j.jfluchem.2020.109692>  
Reference: FLUOR 109692

To appear in: *Journal of Fluorine Chemistry*

Received Date: 21 October 2020  
Revised Date: 18 November 2020  
Accepted Date: 18 November 2020

Please cite this article as: { doi: <https://doi.org/>

This is a PDF file of an article that has undergone enhancements after acceptance, such as the addition of a cover page and metadata, and formatting for readability, but it is not yet the definitive version of record. This version will undergo additional copyediting, typesetting and review before it is published in its final form, but we are providing this version to give early visibility of the article. Please note that, during the production process, errors may be discovered which could affect the content, and all legal disclaimers that apply to the journal pertain.

© 2020 Published by Elsevier.

## Laser Induced Dielectric Breakdown for Synthesis of Chlorofluorosilanes

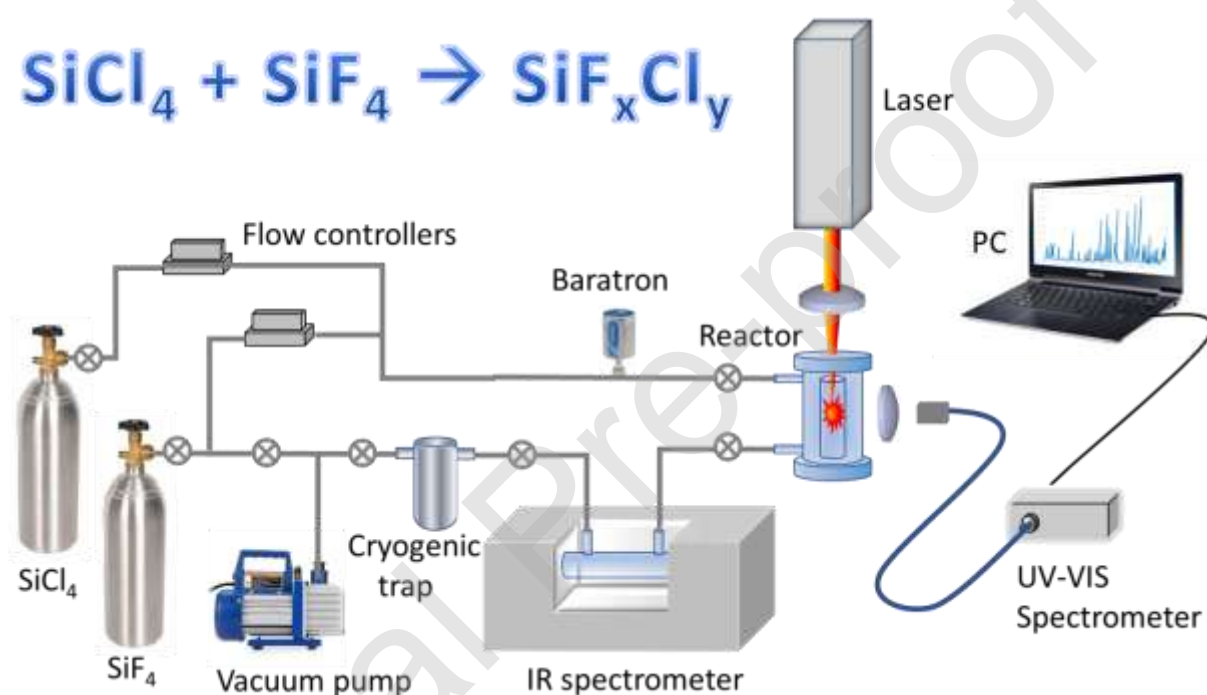
P. G. Sennikov<sup>1</sup>, I. B. Gornushkin<sup>2\*</sup>, A. A. Ermakov<sup>1</sup>, R. A. Kornev<sup>1</sup>, V.E. Shkrinin<sup>1</sup>, V. S. Polyakov<sup>1</sup>

<sup>1</sup>G.G. Devyatikh Institute of Chemistry of High-Purity Substances of RAS, 49 Tropinin Str., Nizhny Novgorod, Russia 603951

<sup>2</sup>BAM Federal Institute for Materials Research and Testing, Richard-Willstätter-Strasse 11, 12489 Berlin, Germany

\*Corresponding author

### Graphical abstract



### Highlights

- Laser induced dielectric breakdown in  $\text{SiF}_4$  and  $\text{SiCl}_4$  mixture is used for the first time to generate fluorochlorosilanes
- Plasma composition and products of plasma chemical reactions are studied by optical, IR, and mass spectroscopy
- Numerical simulations of plasma equilibrium composition and expansion dynamics are performed
- Good agreement between theoretical and experimental data is demonstrated

## Abstract

Tetrafluorosilane ( $\text{SiF}_4$ ) and tetrachlorosilane ( $\text{SiCl}_4$ ) plasmas have been widely used as a source of either F or Cl for etching silicon or as a source of silicon for deposition of Si-based materials. Using different combinations of F and Cl in molecules of chlorofluorosilane  $\text{SiF}_x\text{Cl}_y$  adds additional flexibility in realization of these processes. Direct synthesis of  $\text{SiF}_x\text{Cl}_{4-x}$  ( $x=1, 2, 3$ ) from  $\text{SiF}_4$  and  $\text{SiCl}_4$  is thermodynamically forbidden under standard conditions. This restriction is removed in low-temperature plasmas studied in this work: a laser induced dielectric breakdown (LIDB) plasma and steady-state inductively-coupled plasma (ICP). The plasmas differ in many respects including energy content, temperature, and electron density that lead to different ionization/excitation states of plasma species, which are observed from plasma optical emission spectra. IR spectroscopy and mass-spectrometry confirm the formation of three chlorofluorosilanes,  $\text{SiF}_3\text{Cl}$ ,  $\text{SiF}_2\text{Cl}_2$ , and  $\text{SiFCl}_3$  that constitute  $\sim 60\%$  in products of LIDB plasma and split 50/50 between  $\text{SiF}_3\text{Cl}$ ,  $\text{SiFCl}_3$  and  $\text{SiF}_2\text{Cl}_2$ . Experimental observations are verified by equilibrium static calculations via the minimization of Gibbs free energy and by dynamic calculations via the chemical-hydrodynamic plasma model of a spherically expanding plasma plume. The both types of calculations qualitatively agree with the results of spectroscopic analysis and reproduce dominant presence of  $\text{SiF}_2\text{Cl}_2$  as the temperature of the gas approaches the room temperature.

**Keywords:** chlorofluorosilanes; Laser induced dielectric breakdown; inductively coupled plasma; equilibrium chemical modeling; chemical-hydrodynamic modeling

## 1. Introduction

Silicon halides  $\text{SiF}_4$  and  $\text{SiCl}_4$  have been widely used in various modern technologies for production of silicon and its structures in the form of bulk samples and thin films. These halides differ significantly in physical and chemical properties (Table 1); for example,  $\text{SiF}_4$  has the higher stability, higher ionization energy, and electron affinity compared to  $\text{SiCl}_4$ .

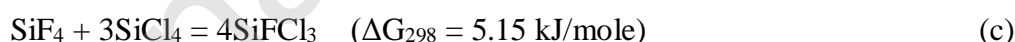
**Table 1** Selected properties of chlorofluorosilanes [1, 2]

Molecule	$t_b, ^\circ\text{C}$	$t_m, ^\circ\text{C}$	$\Delta H_{f,298}, \text{kJ/mol}$	$IE, \text{eV}$	$EA, \text{eV}$	$E_{\text{Si-X}}, \text{eV}$
$\text{SiF}_4$	-95.7	-90	-1609	15.65	-0.46	5.56
$\text{SiF}_3\text{Cl}$	-70.0	-142	-1318	12.03	0.02	
$\text{SiF}_2\text{Cl}_2$	-32.2	-139.7	-1128	12.32	0.39	

SiFCl <sub>3</sub>	12.2	-120.8	-841	12.02	0.52	
SiCl <sub>4</sub>	57.57	-70	-662.8	11.66	0.61	4.69

Plasma-assisted etching and deposition is realized by means of species F, Cl, SiF<sub>x</sub>, and SiCl<sub>x</sub>, which have different chemical activity; therefore a good control is needed over the dissociation of precursor molecules and reaction paths to drive the process toward a desirable result. Filling bonds with either F or Cl in molecules SiF<sub>x</sub>Cl<sub>4-x</sub> (x=0...4) results in large variations in the molecule strength ( $\Delta H_{f298}$ ), ionization energy, and electron affinity (Table 1). This, in turn, provides the smooth change of reactivity of chlorofluorosilanes (depending on the stoichiometric coefficient x) that affects the morphology of deposition layers and the size of crystallites. Fluorosilanes are of interest for inorganic and organic synthesis among other applications. They play a vital role in synthesis of intramolecular hypercoordinate silicon complexes [3] and organosilanes, which are used in organic chemistry as protecting groups and intermediates in organic synthesis [4].

Synthesis of chlorofluorosilanes was first described in [1]. The reaction between SiCl<sub>4</sub> and SbF<sub>5</sub> (using SbCl<sub>5</sub> as a catalyst) was initiated. A similar approach was used later [5, 6] with the reaction between SiF<sub>4</sub> and metal chlorides. Mixed-halogen halo-silanes can also be prepared by the aryl group substitution and halogen exchange [7]. A straightforward method to synthesize chlorofluorosilanes from SiF<sub>4</sub> and SiCl<sub>4</sub> was used in [8] and the corresponding stoichiometric equations are



The small positive Gibbs free energies for these reactions indicate they are not thermodynamically favored under standard conditions, especially the third one. To initiate the reaction, the mixture of gases (b) was heated to 830<sup>0</sup>C [8]. The reaction took place and the condensate, which was collected at -30<sup>0</sup> C was enriched with SiCl<sub>3</sub>F and that, which was collected at -60<sup>0</sup> C was enriched with Si<sub>2</sub>F<sub>2</sub>Cl<sub>2</sub>. Methods of preparation of mixed halo-silanes (containing Cl, Br, I) [7] strongly rely on bonding characteristics of halogens involved. According to Table 1,  $E_{\text{Si-F}} > E_{\text{Si-Cl}}$  that is why F easily replaces Cl and the replacement of first atom is the most favorable. The chlorofluorosilanes SiCl<sub>2</sub>F<sub>2</sub>, SiF<sub>3</sub>Cl, and SiFCl<sub>3</sub> may be separated from other reaction products by low temperature distillation using protocols described, e.g., in [8, 9].

It is interesting to test the feasibility of plasma-chemical reactions (a)-(c) in LIDB plasma and see if they lead to production of chlorofluorosilanes with prescribed chemical compositions. Plasma-chemical approach is used for synthesis of various gaseous, liquid, and solid substances since 1960th [10]. For generation of plasma, single electrons play a decisive role, which always are present in a gas. The electrons accelerate in an electric field that is imposed on the gas and numerous collide with gas species. For plasma generation, only inelastic collisions are important as they lead to excitation and ionization of species. Second and further generations of free electrons (due to ionization) become involved in collisions, form the electron avalanche and, together with other ionized species, the plasma. As a result, active particles such as excited neutral molecules and radicals, atoms, ions and electrons appear in the gas.

To the best of our knowledge, such the “physical” approach has not yet been used for synthesis of chlorofluorosilanes despite the fact that plasma chemical reactions involving  $\text{SiF}_4$ ,  $\text{SiCl}_4$ , and  $\text{H}_2$  were thoroughly studied in different plasma discharges in connection with the manufacturing of Si thin films [11, 12, 13, 14, 15, 16, 17, 18, 19, 20, 21, 22]. A focus of this work is on the use of a very special type of plasma, the LIDB plasma, to initiate chemical reactions and synthesize chlorofluorosilanes.

The phenomenon of laser induced dielectric breakdown (LIDB) was discovered and studied shortly after the invention of a laser in 1958-1960. In 1962, Brech and Cross [23] first observed spectrum from the breakdown plasma, which was initiated by a ruby laser in argon. Since the late 70s, LIDB plasmas have been widely used for analysis of materials [24] but only occasionally for chemical deposition from the gas phase (a so called LIDB-CVD method). First works in this direction were performed by Ronn et al. [25, 26, 27, 28] who initiated the laser breakdown in gaseous  $\text{SF}_6$  and  $\text{UF}_6$ . Only several researchers studied chemical reactions in LIDB plasmas. LIDBs in  $\text{CH}_4$ ,  $\text{CCl}_4$ ,  $\text{CF}_4$  and their mixtures were studied in [26] using optical emission spectroscopy. LIDB was employed in [29] to study pyrolysis of  $\text{C}_1$ – $\text{C}_6$  hydrocarbons and their conversion to acetylene and hydrogen. The by-products  $\text{C}_2\text{H}_4$  and  $\text{CO}_2$  were decomposed into C and  $\text{H}_2$  and CO and  $\text{O}_2$ , correspondingly by the action of the laser radiation. Our group has recently used LIDB for synthesis of boron carbide in the  $\text{BF}_3+\text{CH}_4$  gas mixture [30]. In this connection, it is also worth mentioning the synthesis of  $\text{SiF}_3\text{Cl}$  and  $\text{SiFCl}_3$  by the resonance IR laser decomposition (not LIDB) of  $\text{BCl}_3$  and  $\text{SiF}_4$  molecules [31, 32, 33].

Let us briefly review basic principles of LIDB; its theory was first developed in 1965 by Zel'dovich and Raiser [34]. The optical breakdown occurs when the strength of the electric field in the focused laser beam exceeds the dielectric strength of the gas. Important is presence in the gas of seed free electrons that absorb laser photons (via inverse Bremsstrahlung), ionize gas

molecules and form an electron cascade that leads to formation of plasma. Seed electrons may appear due to multiphoton gas ionization or as a result of random ionization by cosmic radiation. In first several nanoseconds, plasma is opaque absorbing laser energy via inverse Bremsstrahlung; this causes the plasma plume to grow towards the laser beam. The electron temperature of this luminous plasma may reach up to  $10^5$  K and the electron density up to  $10^{17}$ - $10^{19}$   $\text{cm}^{-3}$ . Note the latter is 3-4 orders of magnitude higher than electron densities in plasmas created by electric discharges. Shortly after the laser pulse, plasma loses its energy due to rapid expansion (initially supersonic), radiation, and heat conduction to surroundings. Plasma species (atoms and ions) start emitting discrete radiation several hundreds of nanoseconds past the breakdown. Characteristic molecular spectra appear tens of microseconds later; they originate from molecules of the surrounding gas and molecules that form by association of plasma species. The plasma spectrum contains rich information about types of particles and their concentrations. Shortly after the formation, the LIDB plasma comes to a state close to local thermodynamic equilibrium (LTE). It is logic to assume that transient LIDB plasma can activate chemical processes at least the same efficiently as stationary high-energy plasmas supported by RF discharges, e.g. inductively coupled or microwave.

In this work, we investigate the possibility of synthesis of chlorofluorosilanes  $\text{SiF}_x\text{Cl}_{4-x}$  ( $x = 1, 2, 3$ ) from  $\text{SiF}_4$  and  $\text{SiCl}_4$  using the pulsed LIDB plasma created in the closed-volume reactor. The work consists of three parts. In the first part, equilibrium thermodynamics calculations of  $\text{SiF}_4 + \text{SiCl}_4$  mixtures and dynamic calculations of the expanding plasma plume in these mixtures are performed and discussed. In the second part, optical emission spectra from  $\text{SiF}_4$ ,  $\text{SiCl}_4$  and  $\text{SiF}_4 + \text{SiCl}_4$  LIDB plasmas are analyzed and compared to analogous spectra from inductively coupled plasma. In the third part, the composition of the gas mixtures before and after the laser action is analyzed by IR and mass spectrometry.

## 2. Experimental

Silicon tetrafluoride and tetrachloride of the 99.998% and 99.9999% grades, correspondingly, argon 6N, and hydrogen 5N were used. The experimental setup is shown in Fig.1; it allows the comparative study of both LIDB and ICP plasmas by OES and IR spectroscopy.

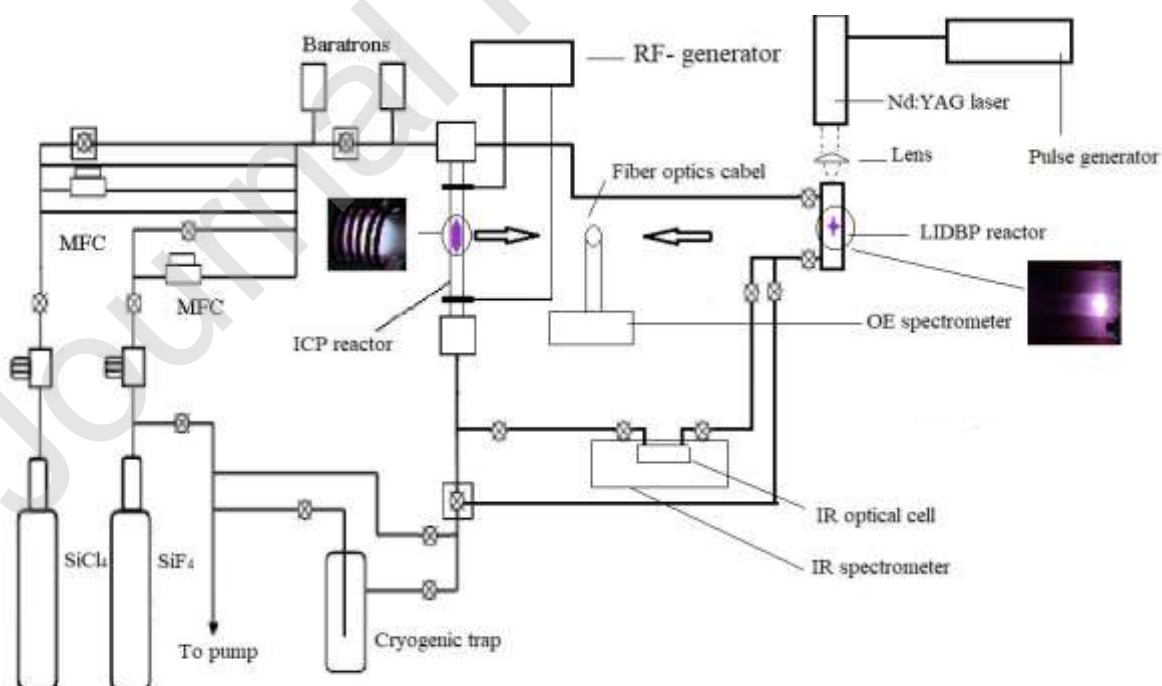
Spectra of pure  $\text{SiF}_4$  and  $\text{SiCl}_4$  in LIDB plasma were recorded at 760 and 240 Torr, correspondingly. LIDB plasma was excited by a pulsed laser in a closed-volume reactor; ICP was excited in a low pressure flow reactor. The compositions and pressures of the gas mixtures used in experiment are given in Table 2.

**Table 2** Composition and pressures of gas mixtures used

Sample #	Gas mixture	Pressure, Torr	Plasma type
1	SiCl <sub>4</sub> : SiF <sub>4</sub> = 1 : 1	460	
2	SiCl <sub>4</sub> : SiF <sub>4</sub> = 1 : 1.61	609	LIDB (expr.)
3	SiCl <sub>4</sub> : SiF <sub>4</sub> = 1 : 2.65	790	
4	SiCl <sub>4</sub> : SiF <sub>4</sub> = 2.65 : 1	760	(calc.)
5	SiCl <sub>4</sub> : SiF <sub>4</sub> = 1 : 1	3	
6	SiCl <sub>4</sub> : SiF <sub>4</sub> = 1 : 0.65	3	ICP (expr.)
7	SiCl <sub>4</sub> : SiF <sub>4</sub> = 1 : 0.35	3	

Unfortunately, it was impossible to using the same gas mixtures at the same pressures in LIDB and ICP plasmas owed to the very large difference in volatility of SiF<sub>4</sub> (gas at room temperature) and SiCl<sub>4</sub> (liquid with vapor pressure of 300 Torr).

The details of the LIDB experiment can be found in [30]. Briefly, a Nd:YAG laser at 1064 nm was used with the 15 ns pulse duration, 800 mJ pulse energy, and 5 Hz repetition rate. The laser was focused inside a cylindrical reactor by a 5 cm focal length lens. The fluence at the focal point was 26 Jcm<sup>-2</sup>. Spectra were detected with a dispersion spectrometer (AvaSpec-ULS3648-USB2-UA-25c) in a spectral range of 200-900 nm with a resolution of 1 nm. The spectrometer worked in a free run mode with the integration time of 50 ms.

**Figure 1** Experimental setup including LIDB and ICP

In experiments with ICP, the reactor was a quartz cylinder placed inside the inductor coil. The coil was connected to a RF generator through an impedance matching device. A smaller cylinder was placed inside the big one and served as a substrate for deposition. A power of the generator was 700 W at a frequency of 13.56 MHz. The gas pressure in the reactor was 3 Torr. The flow of reaction gases SiF<sub>4</sub>, SiCl<sub>4</sub>, and H<sub>2</sub> was regulated in the range of (70-220) ±5 cm<sup>3</sup>/min.

The IR spectra of gaseous components before and after laser irradiation were recorded in a spectral range of 450-7000 cm<sup>-1</sup> by an IR spectrometer (BrukerVertex 80v) and a detector DTGS. The entrance aperture of the spectrometer was 0.5 cm and the resolution was 1 cm<sup>-1</sup>. The gas from the reactor was taken to a cell with the 10 cm optical path; the pressure in the cell was set to 20 Torr.

The quantitative estimation of concentrations of chlorofluorosilanes was carried out using calculated values of integral absorption coefficients of analytical fundamental bands obtained by *ab initio* calculations using the SCF method. The method accounted for electron correlations via the Möller–Plesset perturbation theory (MP2) and quadratic configuration interaction with single and double excitations (QCISD) using the basis sets 6-311G(3df, 3pd) and cc-pVQZ [32, 33].

MS spectra of gaseous components before and after irradiation were measured by a quadrupole mass-spectrometer (ExtorrXT300 (M) SeriesRGA) with the resolution of 1 amu. The working pressure of the analyte gas was between 10<sup>-6</sup>-10<sup>-5</sup>Torr and the residual pressure inside the spectrometer was 5·10<sup>-8</sup>Torr.

### 3. Results

#### 3.1 Equilibrium plasma composition

Equilibrium plasma calculations were carried out in a temperature range of 300-6000K and pressure of 760Torr for the gas mixtures 1, 3, and 4 (Table 2); mixture 4 that was not studied experimentally. The calculations were performed by minimizing the Gibbs free energy of the chemical system under the assumption of local thermodynamic equilibrium (LTE) [37]. Thermodynamic functions of chlorofluorosilanes were calculated using the W1U method [38] that is one of the most accurate composite methods providing the mean absolute deviation for test cases of only~ 0.5 kcal mol<sup>-1</sup>. The calculation results are shown in Tables 3 and 4 along with several experimental data found in literature. In all further calculations, the experimental data were preferred.

**Table 3** Thermodynamic parameters of chlorofluorosilanes calculated by method [38] <sup>a</sup>; in parentheses, the existing experimental data are listed.

SiF <sub>2</sub> Cl	SiFCl <sub>2</sub>	SiF <sub>2</sub> Cl <sub>2</sub>	SiF <sub>3</sub> Cl	SiFCl <sub>3</sub>
---------------------	--------------------	----------------------------------	---------------------	--------------------

$\Delta_f H^{298.15}$ , kJ mol <sup>-1</sup>	-629.9	-424.9	-1132.8	-1372.9 (-1318) <sup>b,c</sup>	-895.3 (-841) <sup>c</sup>
$C_p^{298.15}$ , J mol <sup>-1</sup>	64.2	62.9	82.5	78.2	86.8
$S^{298.15}$ , Jmol <sup>-1</sup> K <sup>-1</sup>	305.6	310.1	323.2	307.6 (309) <sup>c</sup>	332.2 (336) <sup>c</sup>
$S^{298.15}$ , Jmol <sup>-1</sup> K <sup>-1</sup>	14.4	16.4	17.5	16.4	18.5

<sup>a</sup> Previous theoretical result of  $\Delta_f H^{298.15}$  for all chlorofluorosilanes calculated by Gaussian-3 (G3) and G3(MP2) methods are given in [2]. Experimental data are from [48]<sup>b</sup> and [49]<sup>c</sup>.

**Table 4** Coefficients  $a_i$  for approximation of temperature dependence of heat capacity  $C_p = \sum_1^7 a_i T^{i-3}$  in two temperature intervals; indices increase from top to bottom and from left to right.

	298.15 – 1000 K		1000 – 6000 K	
SiF <sub>2</sub> Cl	1.171647434D+05	1.737498355D-05	-2.100330761D+05	-2.428724028D-08
	-2.175846379D+03	-1.201164999D-08	-8.476156453D+01	2.709213610D-12
	1.639540333D+01	3.342333819D-12	9.910388879D+00	-9.415719924D-17
	-1.337724164D-02		8.540581331D-05	
SiFCl <sub>2</sub>	1.171646285D+05	1.947650725D-05	-2.100330761D+05	3.895559515D-08
	-2.185821113D+03	-1.088122963D-08	-8.476107710D+01	-5.819814614D-12
	1.812226107D+01	2.283398724D-12	1.016764040D+01	3.262378028D-16
	-1.714196903D-02		-1.202682549D-04	
SiF <sub>2</sub> Cl <sub>2</sub>	1.171646358D+05	1.383373236D-05	-2.500330761D+05	-1.040775125D-07
	-2.185232985D+03	1.160454622D-08	-8.476107710D+01	1.579406856D-11
	1.769581058D+01	-3.842979040D-12	1.268364070D+01	-8.836012365D-16
	-9.158394391D-03		3.006160053D-04	
SiF <sub>3</sub> Cl	1.171648581D+05	1.561942956D-05	-2.903307610D+05	-1.683589222D-07
	-2.165926860D+03	-1.470605793D-08	-8.476141334D+01	2.611728469D-11
	1.679380467D+01	5.159810974D-12	1.248991292D+01	-1.495922471D-15
	-8.392686031D-03		4.785710172D-04	
SiFCl <sub>3</sub>	1.171646280D+05	1.097463905D-05	-2.903307610D+05	2.165517541D-09
	-2.185914772D+03	-7.516760798D-09	-8.476107710D+01	-4.409752191D-13
	1.843759996D+01	2.182249254D-12	1.303506416D+01	3.500206922D-17
	-9.355661202D-03		-8.464574242D-06	

Figures 2, a-c demonstrate the equilibrium compositions for mixtures 1, 3 and 4 in a temperature range 300-6000 K within which most chemical reactions occur. Maximum concentrations of products, such as SiF<sub>x</sub> and SiCl<sub>x</sub>, chlorofluorosilanes SiFCl, SiF<sub>3</sub>Cl, and SiFCl<sub>3</sub> are within 2000-5000K; the maximum concentration of SiF<sub>2</sub>Cl<sub>2</sub> is within 500-2500 K. SiCl<sub>4</sub> completely dissociates at 4000K and SiF<sub>4</sub> at ~5500K. Other radicals containing Si, F and Cl are also present in this mixture between 2000 K and 6000K. Most of these species are detectable in both plasmas by either OES or IR spectroscopy or mass-spectrometry. One sees from Fig.2 that molecules SiFCl<sub>3</sub> and SiFCl<sub>3</sub> and especially SiF<sub>2</sub>Cl<sub>2</sub> form at their highest concentrations between 500 K and 3000 K. This agrees with the experimental result in [11] where reactions in mixture SiF<sub>4</sub>: SiCl<sub>4</sub> = 1: 1 were thermally activated at 1100K.

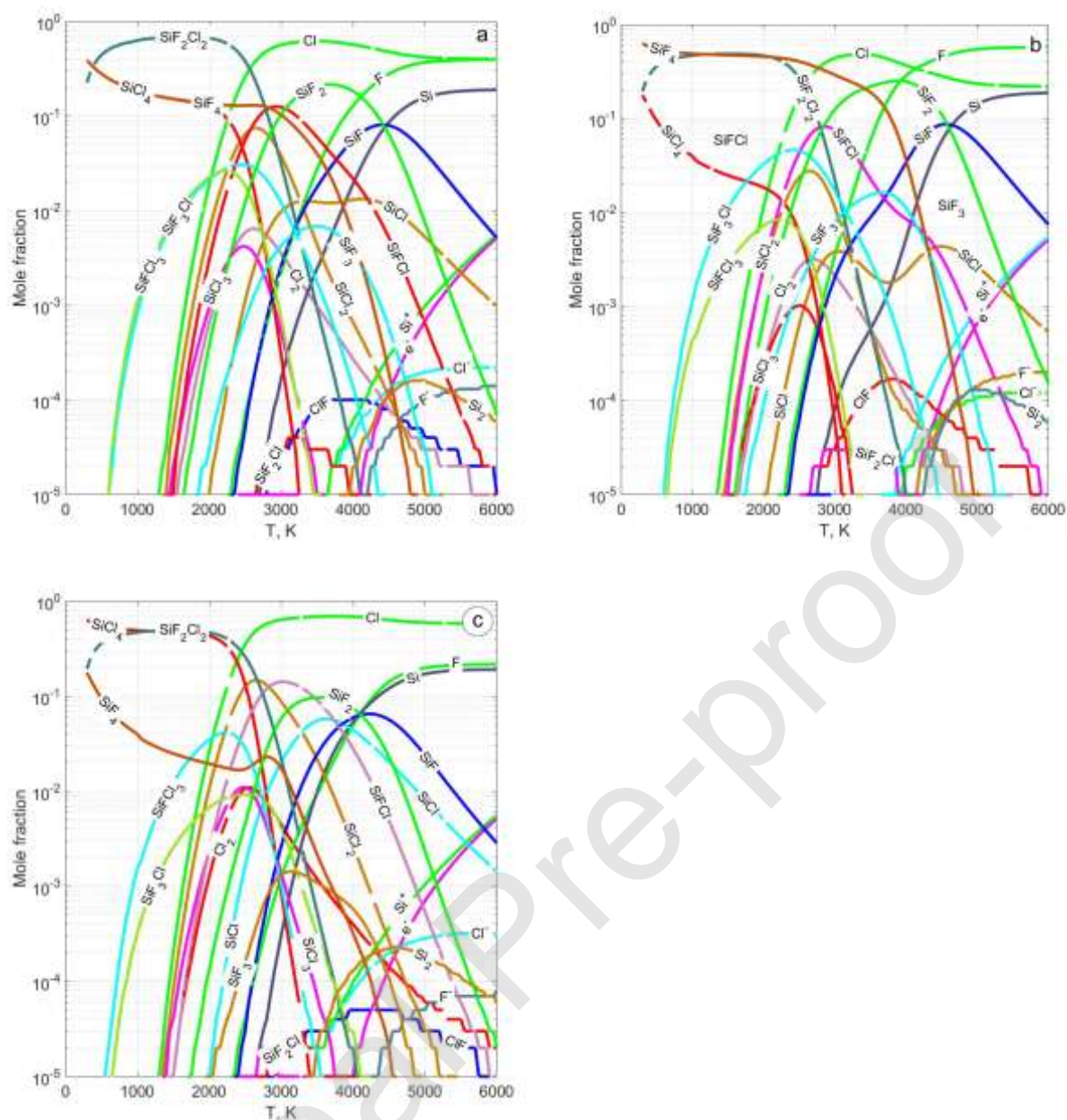


**Figure 2** Equilibrium composition of reaction mixtures: a)  $\text{SiF}_4:\text{SiCl}_4=1:1$ ; b)  $\text{SiCl}_4:\text{SiF}_4=1:2.65$ , and c)  $\text{SiCl}_4:\text{SiF}_4=2.65:1$ ; all at  $P=760\text{Torr}$ .

Note that the values of  $\Delta G_{298}$  for reactions (a) - (c) were obtained based on the thermodynamic functions calculated by us and given in Tables 3 and 4. The corresponding values for higher temperatures are:

**Table 5** Gibbs free energy for reactions (a)-(c) at elevated temperatures

$T, \text{K}$	$\Delta G_T, \text{kJ mol}^{-1}$		
	(a)	(b)	(c)
500	-9.10	-4.50	-5.27
1000	-34.28	-20.79	-31.53

1500      -59.49      -37.13      -57.91

---

In addition to the dependencies in Fig. 2, these data clearly show that reactions (a)-(c) are thermodynamically possible even at relatively low temperatures that is confirmed by the results in [8].

### 3.2 Dynamic simulations

Dynamic calculations of the expanding plasma plume in the  $\text{SiF}_4+\text{SiCl}_4$  gas mixtures are carried out using a fluid dynamic code [41, 42, 43] coupled to an equilibrium chemistry code [44]. The calculations are to see, which fluorochlorosilanes in which plasma zones form during the evolution of the plasma plume. The calculations are performed in the spherical (1D) symmetry. Figure 3 shows the snapshots of plasma thermodynamic parameters, the pressure, temperature, and density at different time instants from 0.1 to 5.0  $\mu\text{s}$ . The initial proportions of gases are given in Table 2 for samples 1, 3, and 4. The calculations are started at the initial temperature of around 5000 K and initial density equal to the density of the gas under normal conditions (room temperature and atmospheric pressure). The entries for both the hydrodynamic code and chemical solver [44] were of a u-v type, i.e. the internal energy – gas density type. The initial internal energy was  $2 \cdot 10^4 \text{ erg cm}^{-3}$  that provided the initial plasma temperature of around 5000 K. The chemical database in [44] was extended by including the calculated and experimental data for 5 new molecules given in Tables 3 and 4.

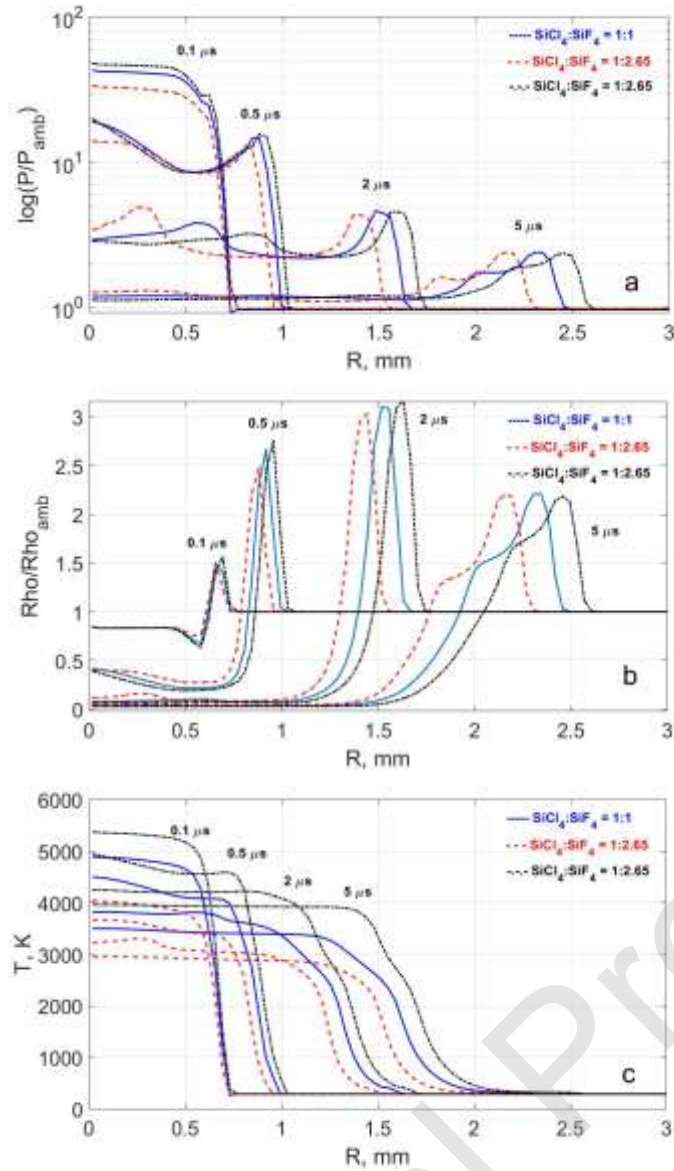


**Figure 3** Expansion dynamics of LIDB plasma at time instants from 0 to 5.0  $\mu\text{s}$ ; a) pressure normalized to ambient pressure (in log scale); b) density (Rho) normalized to ambient density; and c) temperature.

The initial distribution of plasma density was uniform and the initial distribution of internal energy parabolic that simulated a near-Gaussian laser beam profile. The initial plasma radius was 0.6 mm. The numerical convergence was tested and reached at a time step of 1 ns and a spatial step of  $3.8 \cdot 10^{-3}$  cm (the thickness of a spherical layer). Note the initial plasma temperature of  $\sim 5000$  K does not reflect the physical reality. At the onset of laser breakdown the temperature may reach tens of thousands Kelvin. The low initial temperature is chosen to simulate conditions at which molecules form; this saves much computational time. At  $T \gtrsim 5000$  K not much chemistry occurs as only rare molecules survive such the high temperatures. In reality, the temperature around 5000 K sets after  $\sim$ tens of microseconds of plasma evolution; thus a 0-5  $\mu\text{s}$  window in the simulations corresponds to a longer window on a real time scale. Despite the initial plasma conditions are not fully realistic, this does not critically affect the final spatial



SiF<sub>4</sub>:SiCl<sub>4</sub> =1:2.65 mixture; and again of 0.5 in the SiF<sub>4</sub>:SiCl<sub>4</sub>=2.65:1 mixture. The other two chlorofluorosilanes, SiF<sub>3</sub>Cl and SiFCl<sub>3</sub>, remain at the level of the 0.01 mole fraction in all the mixtures. The maximum concentrations of different chlorofluorosilanes are reached at slightly different spatial locations that are determined by the  $T - P$  conditions in those locations. By comparing Fig.3 and 4 one infers that  $P$  in locations, where chlorofluorosilane show the maximum concentrations (at  $R \approx 1.5 - 1.7 \text{ mm}$ ), is almost equal to the ambient pressure, i.e. 1 atm (panel *a* in Fig.3), and  $T$  varies within a narrow corridor around 1000 K (panel *c* in Fig.3). This is consistent with the results of static equilibrium calculations shown in Fig.2, a-c. Thus, the type and amount of chlorofluorosilanes can be regulated by two parameters: the stoichiometry of a gas mixture and plasma temperature.

### 3.3 Optical emission spectra from LIDB plasma in pure SiF<sub>4</sub> and SiCl<sub>4</sub>

The emission spectra of LIDB plasma of pure SiF<sub>4</sub>, SiCl<sub>4</sub> at 760 and 240 Torr correspondingly are shown in Fig. 5. The large FWHMs (full width at half maximum) of lines and bands in the spectrum are due to both the high pressure in the reactor, low resolution of the spectrometer, and long integration time over the entire plasma lifetime. The latter means that spectral lines from atoms and ions at the early “hot” plasma stage overlap with that at the late “cold” plasma stage; besides, bands from molecules and molecular radicals add at the late stage. The spectra are taken at the ~10 s time after the laser irradiation has started. Atomic and molecular lines and bands are assigned using [45, 46]. Both spectra from SiF<sub>4</sub> and SiCl<sub>4</sub> contain intense lines of Si I and Si II at 243.515, 252.611, 288.158, 385.602, 390.552, 413.089, 505.598, and 634.710 nm. Besides, the spectrum of SiF<sub>4</sub> contains the strong band of radical SiF at 439.71 nm ( $A^2\Sigma^+ - X^2\Pi$ ) and the weaker bands at 270-310 nm and 336.3 nm.

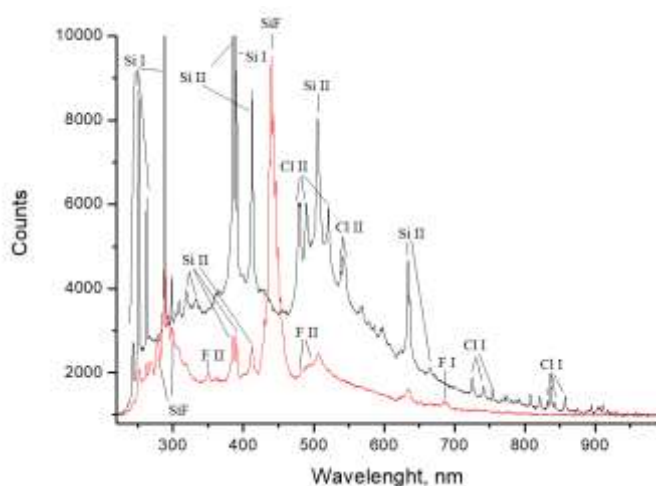


**Figure 5** OES spectrum of pure SiF<sub>4</sub> (red) and SiCl<sub>4</sub> (black) in LIDB plasma

The spectrum of SiF<sub>4</sub> contains weak lines of F I and F II while the SiCl<sub>4</sub> spectrum contains strong lines of Cl I and Cl II. It is also important that SiCl<sub>4</sub> emission spectrum from LIDB plasma does not contain bands from radicals SiCl<sub>x</sub> whose presence is typical for steady-state RF and MW plasmas [47, 48]. This is likely due to the complete dissociation of weak (relative to SiF<sub>4</sub>) molecules of SiCl<sub>4</sub>. This also explains the significantly higher intensity of the emission spectrum of SiCl<sub>4</sub> as compared to SiF<sub>4</sub> even though the SiCl<sub>4</sub> spectrum was detected at twice the lower reactor pressure.

### 3.4 Optical emission spectra of LIDB plasma of SiF<sub>4</sub> and SiCl<sub>4</sub> mixtures

Fig.6, a-b demonstrates the OES spectra of samples 1-3 from LIDB plasma. Since the pressures of the mixtures were different (Table 2) we can only qualitatively discuss main spectral features. Obviously, the spectra are the superposition of the spectra from pure SiF<sub>4</sub> and SiCl<sub>4</sub>; no new lines and bands appear. Several features are worth to note when comparing the spectra from pure SiF<sub>4</sub> and from SiCl<sub>4</sub>. First, the total intensity of the SiCl<sub>4</sub> spectrum increases; second, the intensity ratio  $I(\text{SiF})/I(\text{Si}) = I(439 \text{ nm})/I(288 \text{ nm})$  changes. It decreases from 2 in SiF<sub>4</sub> to 0.65 in SiF<sub>4</sub>+SiCl<sub>4</sub>. With the further increase of the SiF<sub>4</sub> fraction in the SiCl<sub>4</sub>:SiF<sub>4</sub> = 1:2.65 mixture, the ratio decreases to 0.4. The addition of SiCl<sub>4</sub> plays a crucial role in increasing the degree of dissociation of SiF<sub>4</sub> and the number of Si atoms. Many lines from Cl I and Cl II are registered in the region 500-900 nm. To resume, formation of molecules of chlorofluorosilanes in LIDB plasma is likely to occur due to direct reactions between chemically active species SiF, Si I and Si II, F I and F II, Cl I and Cl II.

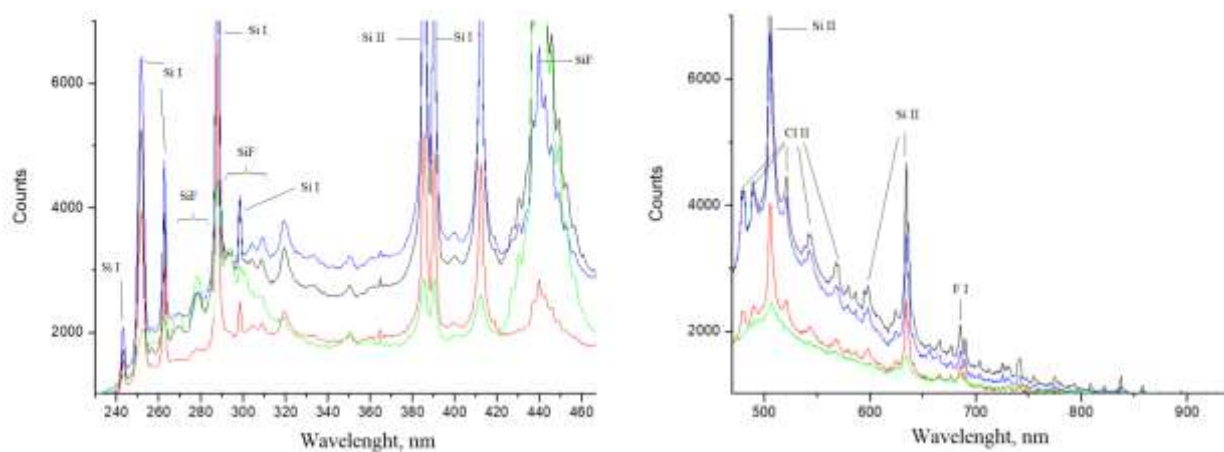


**Figure 6** OES spectra of mixtures of  $\text{SiF}_4$  and  $\text{SiCl}_4$  in LIDB plasma in the spectral range of 240-460 nm (left panel) and 500-900 nm (right panel). Pure  $\text{SiF}_4$  (green),  $\text{SiCl}_4$ :  $\text{SiF}_4=1:1$  (blue);  $\text{SiCl}_4$ :  $\text{SiF}_4=1:1.65$  (black); and  $\text{SiCl}_4$ :  $\text{SiF}_4=1:2.65$  (red)

### 3.5 Optical emission spectra of pure $\text{SiF}_4$ and $\text{SiCl}_4$ in ICP

Differences and similarities in emission spectra from LIDB and ICP plasmas can be seen from the comparison of Fig.5 and 7. Like the LIDB spectra, the overall intensity of the ICP spectrum from pure  $\text{SiCl}_4$  is higher than that from pure  $\text{SiF}_4$ . Lines and bands on the ICP spectrum are narrower owing to the lower reactor pressure (3 Torr). In contrast to LIDB, the ICP spectrum of  $\text{SiCl}_4$  contains fewer lines of Si than the spectrum of  $\text{SiF}_4$ . For the both types of plasmas, the  $\text{SiF}$  band dominates the  $\text{SiF}_4$  spectrum. Like LIDB, no new bands of  $\text{SiF}_x$  are observed in the ICP spectra. But new intense bands of  $\text{SiCl}_x$  are seen in Fig.7, which are assigned according to [46, 47, 48]. Alike with the LIDB spectrum, the ICP spectrum of  $\text{SiCl}_4$  contains strong lines of Cl.

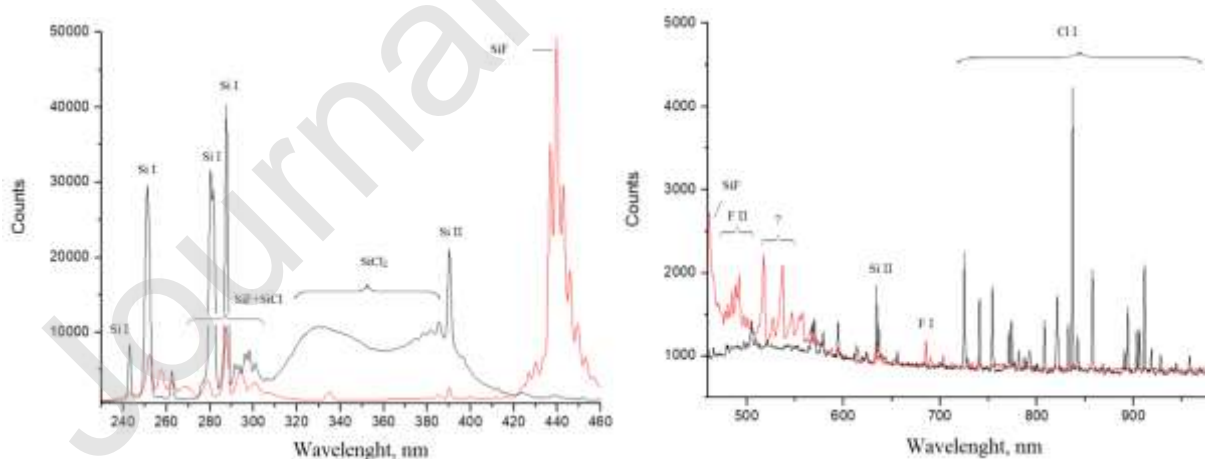


**Figure 7** OES spectra of pure  $\text{SiF}_4$  (red) and  $\text{SiCl}_4$  (black) in ICP; in the spectral range of 240-460 nm (left panel) and 500-900 nm (right panel)

### Optical emission spectra of $\text{SiF}_4$ and $\text{SiCl}_4$ mixtures in ICP

The decreasing trend for SiF<sub>4</sub> in samples 5-7 in ICP (Fig. 8) is the same as in LIDB for samples 3-1 (Fig.6).

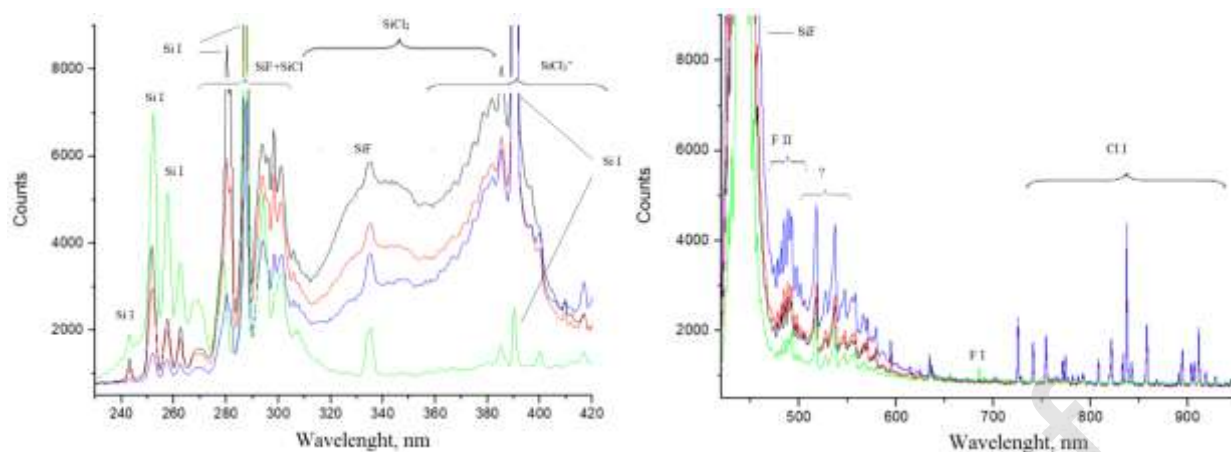


**Figure 8** OES spectra of mixtures of SiF<sub>4</sub> and SiCl<sub>4</sub> in ICP in the range 230-420 nm (left panel) and 450-930 nm (right panel). Pure SiF<sub>4</sub> (green); SiCl<sub>4</sub>:SiF<sub>4</sub>=1:1 (blue); SiCl<sub>4</sub>:SiF<sub>4</sub>=1:0.65 (red), SiCl<sub>4</sub>:SiF<sub>4</sub>=1:0.35 (black)

The characteristic emission bands of SiF at 439 nm and broad bands of SiCl at 280 and 290-310 nm and SiCl<sub>2</sub> at 300-420 nm are seen. Alike with LIDB spectra, bands of SiF<sub>2</sub> and SiF<sub>3</sub> are absent; this point to a large energy content of the ICP discharge. Strong lines of Si I are seen between 250-290 nm, 385-390 nm, and 475-600 nm together with lines of Si II, F I, and F II. These lines are almost absent in the LIDB spectra and are weak in the ICP spectrum of pure SiF<sub>4</sub>. Addition of silicon chloride intensifies radiative processes in this spectral region. Intense lines of Cl I and Cl II appear in a wide region from 700 to 950 nm. In contrast to the LIDB spectrum of SiCl<sub>4</sub>:SiF<sub>4</sub>=1: N (N ≥ 1), the ICP spectrum of SiCl<sub>4</sub>:SiF<sub>4</sub>=1: M (M ≤ 1) is dominated by the SiF band at 439 nm. The relation  $I(\text{SiF})/I(\text{Si})=I(439\text{ nm})/I(288\text{ nm})>1$  holds for all the three mixtures and yields the maximum value of 17 for M = 1. This mixture also exhibits maximum intensity of SiCl<sub>x</sub> bands. It means that with much lower energy input in ICP as compared to LIDB, the non-dissociated SiF and SiCl<sub>x</sub> radicals are primarily responsible for gas reaction products. Atoms of Si, F, and Cl also take part in chemical reactions in this low pressure plasma.

### 3.6 IR spectroscopy of products of plasma-chemical reactions in LIDB plasma

Equilibrium thermodynamic calculations for mixtures of SiF<sub>4</sub> and SiCl<sub>4</sub> predict formation of three chlorofluorosilanes with maximal concentration in the range of 500-4000 K. IR absorption spectra of reaction products were measured after the gas was irradiated by the laser for 40 min. The post-irradiated gas was taken into the IR cell and the pressure was reduced to several tenths Torr. The same experiment could not be performed in ICP because the reactor was of a flow-type and its pressure was only 3 Torr, too low for IR measurements.

Fig. 9 shows the clear difference between the IR spectra from sample 1 ( $\text{SiF}_4:\text{SiCl}_4=1:1$ ) taken before and after the laser irradiation. The bands of three fluorosilanes appear in spectral ranges close to that of the fundamental bands of  $\text{SiF}_4$  ( $1030\text{ cm}^{-1}$ ) and  $\text{SiCl}_4$  ( $616\text{ cm}^{-1}$ ). All the IR bands are identified using [49]. Similar spectra were obtained for samples 2 and 3. Analytical bands chosen for determination of concentrations of chlorofluorosilanes are given in Table 6.

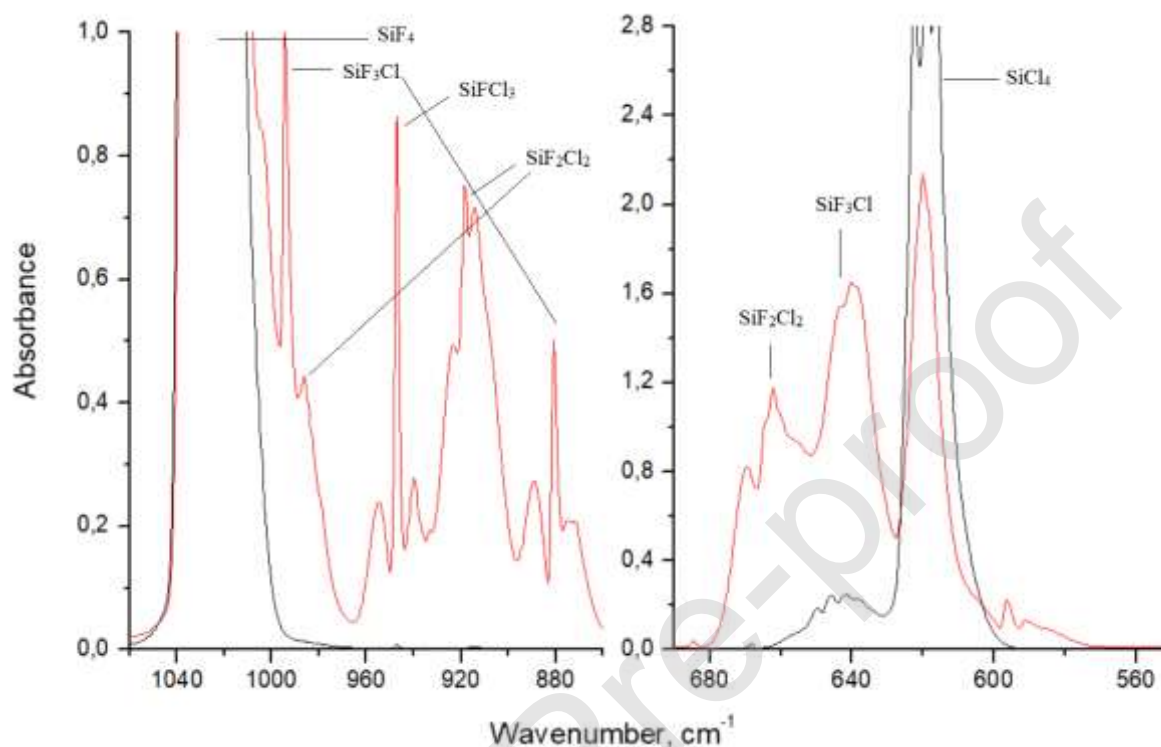


**Figure 9** IR absorption spectra of mixture  $\text{SiCl}_4:\text{SiF}_4=1:1$  before (black) and after (red) irradiation during 40 min.

To find concentrations of chlorofluorosilanes using the Lambert-Beer law, values for integral absorption coefficients of bands were required. The values were calculated *ab initio* using a quantum-chemical method (see Experimental). It follows from the data in Table 6 that chlorofluorosilanes are formed in different proportions and different absolute quantities in mixtures with different content of  $\text{SiF}_4$ . The maximum concentration of chlorofluorosilanes was found in the equimolar mixture (sample 1), i.e. in the mixture with the maximum concentration of  $\text{SiCl}_4$ . The total concentration of fluorosilanes in reaction products exceeds 60% and the concentration of  $\text{SiF}_2\text{Cl}_2$  is the highest among all the mixtures. These experimental data follow qualitatively very well the theoretical predictions (Fig.2, a-c). According to equilibrium thermodynamics,  $\text{SiF}_2\text{Cl}_2$  also dominates all the mixtures while the concentrations of  $\text{SiFCl}_3$  and  $\text{SiF}_3\text{Cl}$  are about two orders of magnitude lower and are close to each other.

**Table 6** Concentrations of chlorofluorosilanes in mol% determined from IR spectra of post-irradiated samples 1-3

Molecule	Band cm <sup>-1</sup> [49]	$A \times 10^8$ cm <sup>2</sup> s <sup>-1</sup>	Sample 1 mol%	Sample 2 mol%	Sample 3 mol%
SiF <sub>2</sub> Cl <sub>2</sub>	915	50	32±3	29±3	17±3
SiFCl <sub>3</sub>	947	12	18±2	12±2	6±1
SiF <sub>3</sub> Cl	876	38	13±2	11±2	6±1
Total			63	52	29

### 3.7 Mass-spectrometry of reaction products in LIDB and ICP

The MS results qualitatively confirm the results obtained by IR spectroscopy of LIDB products. Fig. 10, a demonstrates a part of the mass-spectrum of the SiCl<sub>4</sub>:SiF<sub>4</sub>=1:1 mixture. One sees that the decrease in intensity of ions relevant to SiF<sub>4</sub> (close to 85 M/e) and SiCl<sub>4</sub> (170 M/e) occurs. Simultaneously, new peaks corresponding to fragments of chlorofluorosilane molecules SiFCl<sub>3</sub> and SiF<sub>2</sub>Cl<sub>2</sub> appear. The spectral features in regions of 120 and 135 M/e point to the preferential formation of SiF<sub>2</sub>Cl<sub>2</sub>. Fig. 10, b demonstrates the different concentration levels of SiFCl<sub>3</sub> in three mixtures studied, which agree with the IR data in Table 6. The concentration of SiFCl<sub>3</sub> is maximal in the equimolar mixture and minimal in mixture 3 with excess of SiF<sub>4</sub>.

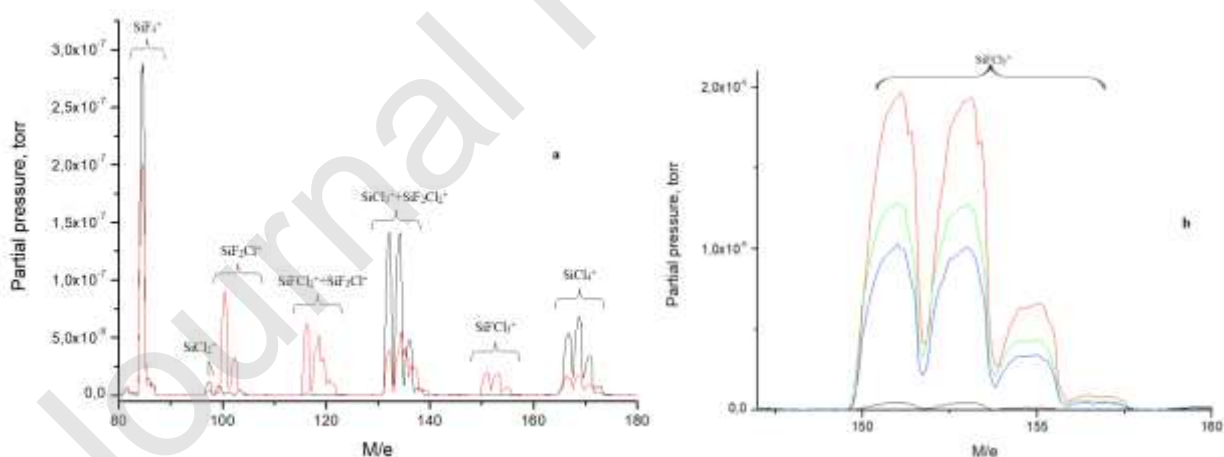


**Figure 10** a) Mass-spectrum of the SiF<sub>4</sub>:SiCl<sub>4</sub>=1:1 LIDB mixture before (black) and after (red) laser irradiation; b) zoomed range 145-160 M/e: SiCl<sub>4</sub>=1:1 before (black) and after (red) laser irradiation; SiCl<sub>4</sub>:SiF<sub>4</sub>=1:1.65 (green) and SiCl<sub>4</sub>:SiF<sub>4</sub>=1:2.65 (blue) after laser irradiation.

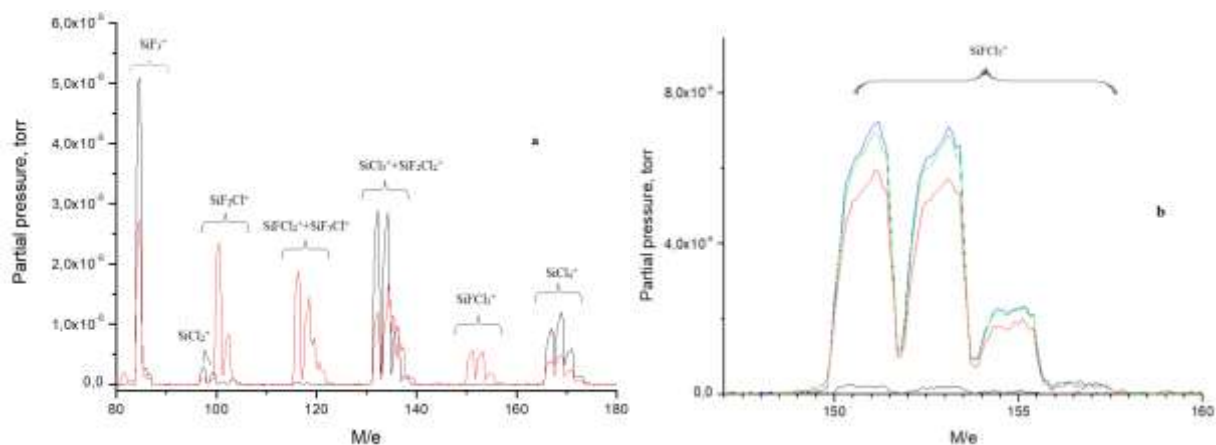


**Figure 11** a) Mass-spectra of the  $\text{SiF}_4:\text{SiCl}_4=1:1$  ICP mixture before (black) and after (red) ICP exposure; b) zoomed range 145-160 M/e:  $\text{SiF}_4:\text{SiCl}_4=1:1$  before (black) and after (red) ICP exposure;  $\text{SiCl}_4:\text{SiF}_4=1:0.65$  (green) and  $\text{SiCl}_4:\text{SiF}_4=1:0.35$  (blue) mixtures after ICP exposure.

Fig.11, a demonstrates the mass-spectrum of the  $\text{SiF}_4:\text{SiCl}_4=1:1$  mixture before and after the steady-state ICP exposure. This mass-spectrum differs from that in Fig.10, a of the LIDB products by only the partial pressure values on the ordinate axis. It means that chlorofluorosilanes form also in ICP and Cl-enriched molecules are the most favored. It is confirmed by Fig.11, b where the intensities of the  $\text{SiFCl}_3^+$  ion in different mixtures are compared. Despite small differences in values of intensities, one sees that in the 1:1 mixture the concentration of  $\text{SiFCl}_3$  is lower than that in the enriched by  $\text{SiCl}_4$  mixture 7.

#### 4. Discussion

According to the equilibrium thermodynamic calculations, the formation of molecules of  $\text{SiF}_x\text{Cl}_{4-x}$  ( $x=1,2,3$ ), which reach the maximal concentrations between 1000-3000K is possible by chemical reactions between fragments of  $\text{SiF}_4$  and  $\text{SiCl}_4$  molecules. The direct reaction between  $\text{SiF}_4$  and  $\text{SiCl}_4$  is thermodynamically forbidden under standard conditions but favored starting from at least 500K. The formation of  $\text{SiF}_2\text{Cl}_2$  seems to be preferred in all the cases at low temperatures around 1000 K. The inspection of the concentration-vs-temperature dependence of the reaction products shows that mixtures  $\text{SiF}_4+\text{SiCl}_4$  with higher initial concentrations of  $\text{SiCl}_4$  produce more  $\text{SiFCl}_3$  than  $\text{SiF}_2\text{Cl}_2$ . In mixtures with higher initial  $\text{SiF}_4$ , the production of  $\text{SiF}_3\text{Cl}$  is favored. To study the plasma-activated reaction between  $\text{SiCl}_4$  and  $\text{SiF}_4$ , we used two types of plasma: LIDB (for the first time) and ICP. The plasmas differ in energy content ( $60 \text{ J cm}^{-3}$  and  $8 \text{ J cm}^{-3}$ , correspondingly) that led to different plasma composition and, hence, different reaction chemistry. For LIDB, we used a closed-volume reactor with the pressure of reacting gases reaching several hundreds of Torr; the plasma was close to LTE at a stage of molecule formation. For ICP, the flow reactor type was used with the pressure of 3 Torr; the plasma here was essentially non-equilibrium. In both plasmas, however, chlorofluorosilanes have formed.

That was confirmed by IR (for LIDB) and MS (for both LIDB and ICP) measurements. Optical emission spectroscopy (OES) revealed the high degree of dissociation of mixture components in LIDB plasma. Only one molecular radical, SiF, has formed. The intensity of its emission band (proportional to the concentration) decreased abruptly as SiCl<sub>4</sub> was added to SiF<sub>4</sub> accompanied by the increase in the intensity of Si lines. No radicals SiCl<sub>x</sub> were observed by OES. The IR absorption spectroscopy of post-reaction products showed, however, the presence of all three chlorofluorosilanes with the maximal concentration found in the equimolar SiCl<sub>4</sub>+SiF<sub>4</sub> mixture (the highest in SiCl<sub>4</sub> content among all the mixtures studied). Out of three chlorofluorosilanes, SiF<sub>2</sub>Cl<sub>2</sub> was the most abundant, in full agreement with the prediction of the equilibrium model. The trend toward the decreasing yield of chlorofluorosilanes with decreasing amount of SiCl<sub>4</sub> and the dominance of SiF<sub>2</sub>Cl<sub>2</sub> was observed for other mixtures too. The MS measurements have qualitatively confirmed these results.

In the low-pressure ICP, the formation of SiCl<sub>x</sub> radicals was observed. The MS measurements confirmed the formation of three chlorofluorosilanes with the maximal concentrations detected in the mixture with the highest concentration of SiCl<sub>4</sub> (i.e. SiF<sub>4</sub>: SiCl<sub>4</sub>=0.35:1).

The study has demonstrated that thermodynamically controlled formation of chlorofluorosilanes from SiF<sub>4</sub> and SiCl<sub>4</sub> is possible in plasmas of markedly different nature (ICP and LIDB) through possibly different chemical mechanisms. Two most abundant chlorofluorosilanes observed experimentally were SiF<sub>2</sub>Cl<sub>2</sub> and SiFCl<sub>3</sub>. The equilibrium model predicted the same. From the perspective of formation enthalpies and bonding energies of SiF<sub>4</sub> and SiCl<sub>4</sub> (see Table 1) the replacement of one chlorine atom by fluorine atom (but not the reverse) is the most thermodynamically favored process under true thermal equilibrium conditions. In LIDB plasma under LTE, the replacement of two chlorine atoms by two fluorine atoms must be the most favored process that occurs by means of collisions between highly energetic species. That is what was observed experimentally. The formation of SiF<sub>3</sub>Cl at relatively high concentrations is also possible.

To resume, our study showed that LIDB plasma ignited in a closed-volume reactor at pressures close to atmospheric can be an effective method of production of chlorofluorosilanes from SiCl<sub>4</sub> and SiF<sub>4</sub>. In our experiments, a total yield of all chlorofluorosilanes in LIDB plasma reached 60%. This experimental result agrees with the result of dynamic simulations, which show that production of chlorofluorosilanes (especially SiF<sub>2</sub>Cl<sub>2</sub>) in peripheral plasma zones is indeed very efficient.

## 5. Conclusions

1. Chlorofluorosilanes  $\text{SiF}_3\text{Cl}$ ,  $\text{SiF}_2\text{Cl}_2$ ,  $\text{SiFCl}_3$  were synthesized for the first time by laser-induced dielectric breakdown (LIDB) and by inductively coupled plasma (ICP) from the mixtures of  $\text{SiF}_4$  and  $\text{SiCl}_4$  at pressures of several hundred and 3 Torr, correspondingly. The high pressure transient LIDB plasma was close to local thermodynamic equilibrium (LTE) at the stage of molecule formation whereas the low-pressure steady-state ICP was substantially non-equilibrium.
2. Optical emission spectra from both the LIDB and ICP plasmas were studied and it was found that the dissociation of  $\text{SiCl}_4$  in LIDB plasma was almost complete. The dissociation of  $\text{SiF}_4$  resulted in the  $\text{SiF}$  radical; Si and F atoms, and their ions. The dissociation of both halides in ICP resulted in the formation of radicals  $\text{SiF}$ ,  $\text{SiCl}$  and  $\text{SiCl}_2$  and atomic and ionic species of Si, F and Cl. This points to different reaction mechanisms of formation of chlorofluorosilanes in the two plasmas.
3. It was shown by IR and mass spectroscopy that yield of chlorofluorosilanes in both plasmas was the highest for mixtures with the highest concentration of  $\text{SiCl}_4$ . According to the IR data, the total yield of chlorofluorosilanes in LIDB plasma comprised 60%, with ~30% of  $\text{SiF}_2\text{Cl}_2$
4. The equilibrium thermodynamic model adequately predicted the composition of both the LIDB and ICP plasmas. It predicted that the most abundant chlorofluorosilane is  $\text{SiF}_2\text{Cl}_2$  as was also confirmed by experiment.
5. The dynamic calculations of the expanding plasma plume agreed well with experiment and showed that chlorofluorosilanes form in the peripheral plasma zone of the LIDB plasma and are sensitive to the mixture stoichiometry and plasma temperature.

### Conflict of interests

The authors report no conflict of interests in regard to this manuscript.

### Acknowledgments

The authors thank Prof. U. Panne and Dr. K. Rurack for support of this project. P.S., R.A. and A.A. acknowledge the RSF grant No 20-13-00035 for basic support as well as the Russian Ministry of Education and Science (subject 0095-2019-0008) for the partial support. The authors are grateful to Melsytech LTD (D.Stepanov, A.Stepanov, O.Yeremeykin) for technical support.

## References

- [1] H.S. Booth, C.F. Swinehart, The chlorofluorosilanes, *J. Amer. Chem. Soc.* 57 (1935) 1333-1337.
- [2] S.-Y. Chien, W.-K. Li, N.L. Ma, Thermochemistry of hydrochlorofluorosilanes: a Gaussian-3 study, *J. Phys. Chem. A* 104 (2000) 11398-11402.
- [3] A.A. Nikolin, V.V. Negrebetsky, Synthesis, properties and reactivity of intramolecular hypercoordinate silicon complexes, *Russian Chem. Rev.* 83 (2014) 848-883.
- [4] <https://www.thermofisher.co.nz/Uploads/file/Acros-Organosilanes-whitepaper.pdf> (accessed on 18 November 2020).
- [5] M. Schmeisser, H. Jenkner, Zur Kenntnis anorganischer Säurefluoride (I), *Z. Naturforschung B: Anorg. Chem. Org. Chem.* 7 (1952) 191-192.
- [6] B.W.C. Schumb, D.W. Breck, Some metathetical reactions of the gaseous fluorides of group IV, *J. Amer. Chem. Soc.* 74 (1952) 1754-1760.
- [7] E. Asirvatham, J. Czarnecki, M.H. Luly, L.F. Mullan. A. Thenappan, Preparation of mixed-halogen halo-silanes, United States Patent (2006) 7030260 B2.
- [8] R.V. Lindsey, Preparation and reactions of dichlorofluorosilane, *J. Amer. Chem. Soc.* 73 (1951) 371-373.
- [9] F.T. Fitch, P.C. Miller, Preparation of fluorosilanes, United States Patent (1958) 2865706.
- [10] F.B. Vurzel, L.S. Polak, Plasma-chemical technology – the future of the chemistry industry, *Ind. Eng. Chem.* 62 (1970) 8-22.
- [11] G. Bruno, P. Capezzuto, G. Cicala, Rf glow discharge of SiF<sub>4</sub>-H<sub>2</sub> mixtures: diagnostics and modeling of the a-Si plasma deposition process, *J. Appl. Phys.* 69 (1991) 7256-7266.
- [12] G. Bruno, P. Capezzuto, G. Cicala, Novel approaches to plasma deposition of amorphous silicon-based materials, *Pure Appl. Chem.* 64 (1992) 725-730.
- [13] G. Cicala, G. Bruno, P. Capezzuto, Plasma deposition of amorphous silicon alloys from fluorinated gases, *Pure Appl. Chem.* 68 (1996) 1143-1149.
- [14] P. Roca I Cabarrocas, Plasma enhanced chemical vapor deposition of amorphous, polymorphous and microcrystalline silicon films, *J. Non-Cryst. Solids*, 266-269 (2000) 31-37.
- [15] S. Kasout, S. Kumar, R. Vanderhaghen, P. Roca I Cabarrocas, I. French, Fluorine and hydrogen effects on the growth and transport properties of microcrystalline silicon from SiF<sub>4</sub> precursor, *J. Non-Cryst. Solids* 299-302 (2002) 113-117.
- [16] J.-C. Dornstetter, J. Wang, B. Bruneau, E.V. Johnson, P. Roca I Cabarrocas, Material and growth mechanism studies of microcrystalline silicon deposited from SiF<sub>4</sub>/H<sub>2</sub>/Ar gas mixtures, *Can. J. Phys.* 92 (2014) 740-743.

- [17] J.-C. Dornstetter, B. Bruneau, P. Bulkin, E.V. Johnson, P. Roca I Cabarrocas, Understanding the amorphous-to-microcrystalline silicon transition in SiF<sub>4</sub>/H<sub>2</sub>/Ar gas mixtures, *J. Chem. Phys.* 140 (2014) 234706.
- [18] A.V. Vodopyanov, S.V. Golubev, D.A. Mansfeld, P.G. Sennikov, Experimental investigations of silicon tetrafluoride decomposition in ECR discharge plasma, *Rev. Sci. Instrum.* 82 (2011) 063503.
- [19] P. Sennikov, D. Pryakhin, N. Abrosimov, B. Andreev, Yu. Drozdov, M. Drozdov, A. Kuznetsov, A. Murel, H.-J. Pohl, H. Riemann, V. Shashkin, PECVD growth of crystalline silicon from its tetrafluoride, *Cryst. Res. Technol.* 45 (2010) 899- 908.
- [20] P.G. Sennikov, A.V. Vodopyanov, S.V. Golubev, D.A. Mansfeld, M.N. Drozdov, Yu.N. Drozdov, B.A. Andreev, L.V. Gavrilenko, D.A. Pryakhin, V.I. Shashkin, O.N. Godisov, A.I. Glasunov, A.Ju. Safonov, H.-J. Pohl, M.L.W. Thewalt, P. Becker, H. Riemann, N.V. Abrosimov, S. Valkiersi, Towards 0.99999 <sup>28</sup>Si, *Solid State Commun.* 152 (2012) 455-460.
- [21] D.A. Mansfeld, A.V. Vodopyanov, S.V. Golubev, P.G. Sennikov, L.A. Mochalov, B.A. Andreev, Yu.N. Drozdov, M.N. Drozdov, V.I. Shashkin, P. Bulkin, P.Roca I Cabarrocas, Deposition of microcrystalline silicon in electron-cyclotron resonance discharge (24 GHz) plasma from silicon tetrafluoride precursor, *Thin Solid Films* 562 (2014) 114-117.
- [22] P.G. Sennikov, R.A. Kornev, L.A. Mochalov, S.V. Golubev, PECVD preparation of silicon and germanium with different isotopic composition via their tetrafluorides, *J. Phys. Conf. Ser.* 514 (2014) 012002.
- [23] F. Brech, L. Cross, Optical microemission stimulated by a ruby laser, *Appl. Spectrosc.* 16 (1962) 59.
- [24] L.J.Radziemski, From LASER to LIBS, the path of technology development, *Spectrochim. Acta B* 57 (2002) 1109-1113.
- [25] A.M. Ronn, B.L. Earl, Laser induced dielectric breakdown studies of the reaction UF<sub>6</sub> + H<sub>2</sub>, *Chem. Phys. Lett.* 45 (1977) 556-558.
- [26] A.H. Schwebel, A.M. Ronn, Spectroscopy of laser-induced dielectric breakdown in gas mixtures, *Chem. Phys. Lett.* 100 (1983) 178-182.
- [27] S.T. Linn, A.M. Ronn, Laser induced sulfur particulate formation, *Chem. Phys. Lett.* 56 (1978) 414-418.
- [28] A.M. Ronn, Particulate formation induced by infrared laser dielectric breakdown, *Chem. Phys. Lett.* 42 (1976) 202-204.
- [29] H. Kojima, K.Naito, High-temperature pyrolysis by laser gas breakdown, *Ind. Eng. Chem. Prod. Res. Dev.* 20 (1981) 396-399.

- [30] I.B. Gornushkin, P.G. Sennikov, R.A. Kornev, A.A. Ermakov, V.E. Shkrinin, Laser induced dielectric breakdown for chemical vapor deposition by hydrogen reduction of volatile boron halides  $\text{BCl}_3$  and  $\text{BF}_3$ , *Plasma Chem. Plasma Process* 40 (2020) 1145-1162.
- [31] N.G. Basov, A.N. Oraevskij, A.V. Pankratov, Kinetics of “laser-chemical” reactions, *Soviet J. Quant. Electr.* 6 (1976) 443-448.
- [32] Y. Adamova, A. Pankratov, V. Sagit, A. Skachkov, G. Stolyarova, G. Shmerling, Laser chemical reaction of boron trichloride with silicon tetrafluoride, *Khimia Vysokih Energij* 12 (1978) 89-90 (in Russian).
- [33] Y. Adamova, A. Skachkov, Reaction of boron trichloride with tetrafluorosilane initiated by two frequency-tunable carbon dioxide lasers, *Khimia Vysokih Energij* 24 (1990) 88-91 (in Russian).
- [34] Ya.B. Zeldovich, Yu.P. Raizer, *Physics of shock waves and high-temperature hydrodynamic phenomena*, Dover Publ., N.Y. 2002.
- [35] A.P. Burtsev, V.N. Bocharov, S.K. Ignatov, T.D. Kolomicetsova, P.G. Sennikov, K.G. Tokhadze, L.A. Chuprov, D.N. Shchepkin, O. Schrems, Integral intensities of absorption bands of silicon tetrafluoride in the gas phase and cryogenic solution: experiment and calculation, *Opt. Spectrosc.* 98 (2005) 227-234.
- [36] N.C. Handy, J.F. Gaw, E.D. Simandiras, Accurate ab initio prediction of molecular geometries and spectroscopic constants, using SCF and MP2 energy derivatives, *J. Chem. Soc., Faraday Trans.* 83 (1987) 1577-1593.
- [37] G.V. Belov, V.S. Iorish, V.S. Yungman, Simulation of equilibrium states of thermodynamic systems using IVTANTERMO for Windows, *High Temp.* 38 (2000) 191-196.
- [38] S. Parthiban, J.M.L. Martin, Assessment of W1 and W2 theories for the computation of electron affinities, ionization potentials, heats of formation, and proton affinities, *J. Chem. Phys.* 114 (2001) 6014-6029.
- [39] M.W. Chase, Jr., C.A. Davies, J.R. Downey, Jr, D.J. Frurip, R.A. McDonald, A.N. Syverud, *JANAF Thermochemical Tables, 3rd Ed., Part I, Al-Co*, *J. Phys. Chem. Ref. Data* 14 (1985) Suppl. 1.
- [40] C. L. Yaws, *Yaws Handbook of Thermodynamic Properties for Hydrocarbons and Chemicals*, Gulf Publ. Company, 2007.
- [41] S. Shabanov, I. Gornushkin, Chemistry in laser-induced plasma at local thermodynamic equilibrium, *Appl. Phys. A* 124 (2018) 716.
- [42] S.V. Shabanov, I.B. Gornushkin, Modeling chemical reactions in laser induced plasma, *Spectrochim. Acta B* 100 (2014) 147-172.
- [43] S. Shabanov, I. Gornushkin, Anions in laser induced plasmas, *Appl. Phys. A* 122 (2016)

676.

[44] <https://cearun.grc.nasa.gov> (accessed on 18 November 2020)

[45] A. Kramida, Yu. Ralchenko, J. Reader, and NIST ASD Team (2020), NIST Atomic Spectra Database, <https://physics.nist.gov/asd> (accessed on 18 November 2020).

[46] R.W.B. Pearse, A.G. Gaydon, The identification of molecular spectra, Chapman and Hall, London, 1976.

[47] G. Bruno, P. Capezzuto, G. Cicala, F. Cramarossa, Mechanism of silicon film deposition in the RF plasma reduction of silicon tetrachloride, Plasma Chem. Plasma Process 6 (1986) 109-125.

[48] H.-J. Tiller, S. Sameith, Emission spectroscopic investigations on  $\text{SiCl}_4$  and  $\text{CCl}_4/\text{Si}$  plasmas for etching processes, Contrib. Plasma Phys. 30 (1990) 703-713.

[49] K. Hamada, G.A. Ozin, E.A. Robinson, Raman, IR, NMR, and NQR of chlorofluorosilanes, Bull. Chem. Soc. Japan 44 (1971) 2555-2556.